



Cite this: *Chem. Commun.*, 2016,  
52, 10411

Received 17th May 2016,  
Accepted 26th July 2016

DOI: 10.1039/c6cc04155h

[www.rsc.org/chemcomm](http://www.rsc.org/chemcomm)

## Endohedral dynamics of push–pull rotor-functionalized cages†

Marcel Krick,<sup>a</sup> Julian Holstein,<sup>a</sup> Christian Würtele<sup>b</sup> and Guido H. Clever<sup>\*a</sup>

**A series of  $[Pd_2L_4]$  coordination cages featuring endohedral functionalities in central backbone positions was synthesized. Although attached via  $C=C$  double bonds, the substituents behave as molecular rotors. This is explained by their pronounced donor–acceptor character which lowers rotational barriers and allows for electronic control over the spinning rates inside the cage. The dynamic behaviour of the free ligands, assembled cages and host–guest complexes is compared with the aid of NMR experiments, X-ray structure analysis and molecular modelling.**

Confined molecular environments in proteins or folded oligonucleotides are often lined with a combination of rigidly fixed functionalities as well as flexible structural elements, such as dangling loops, amino acid residues or nucleobases.<sup>1</sup> The controlled motion of such flexible attachments may gate the entrance of substrates, induce chemical conversions or transmit information in the form of allosteric regulation.<sup>2</sup> In the field of supramolecular assembly, countless nanoscale cavities have been synthesized over the last decades and examined for guest exchange,<sup>3</sup> selective recognition<sup>4</sup> and catalytic conversions.<sup>5</sup> In recent years, strategies for the incorporation of defined functionalities such as redox units,<sup>6</sup> photo switches<sup>7</sup> or specific binding sites have been developed in order to further increase the hosts' capabilities and equip the systems with advanced features such as stimuli-responsiveness,<sup>8</sup> allosteric regulation<sup>9</sup> or tuneable reactivity.<sup>10</sup> Furthermore, the metal-mediated self-assembly of structures such as helicates,<sup>11</sup> entangled architectures<sup>12</sup> and coordination cages<sup>13</sup> has turned out to be a particularly successful strategy for the generation of a large degree of structural and functional variety.<sup>14</sup> Amongst those architectures, the installation of endohedral functionality remains a challenge and only few examples

have been reported including inward-pointing hydrogen bond donors<sup>15</sup> and acceptors,<sup>16</sup> reactive residues inside helicates, cages and spheres,<sup>17,18</sup> organocatalysts,<sup>19</sup> metal-coordination sites,<sup>20</sup> and others.<sup>21</sup>

With respect to the incorporation of dynamic functionality in self-assembled cavities, noteworthy examples from the area of solid materials include rotaxane–MOF hybrids<sup>22</sup> and the family of flexible porous coordination compounds.<sup>23</sup> In the context of discrete self-assemblies, combinations of rings<sup>24</sup> and cages<sup>25</sup> with mechanically interlocked substructures have been reported. We have recently introduced a sterically overcrowded  $[Pd_2L_4]$  host consisting of four ligands carrying bulky adamantyl ligands in a central position that were shown to flip between two degenerate conformations both in the free ligand as well as the assembled cage.<sup>26</sup>

Comparable to our previous dynamic  $[Pd_2L_4]$  system,<sup>26</sup> the one under scrutiny here is synthetically derived from a flat acridone ligand that we have studied before in the context of stimuli responsive double-cages.<sup>27</sup> Herein we report the installation of endohedral groups consisting of two electron-withdrawing substituents (COOR and/or CN) attached to an electron-rich backbone via a  $C=C$  double bond (Fig. 1a).<sup>28</sup> In contrast to the chemical drawing which suggests a totally flat system, steric demands (repulsion between backbone protons and the substituents of the double bond) cause the endohedral group to bend to one side of the backbone (Fig. 1b and 3a–c). Compounds based on the same structural motif have been previously examined as luminescent materials,<sup>29</sup> conductive polymers<sup>30</sup> and EPR labels for DNA.<sup>31</sup> We were interested in the structural dynamics of the system in the context of supramolecular self-assembly, since the push–pull character of the underlying conjugated system (Fig. 1c) was expected to allow for rotation around the  $C=C$  double bond in a kinetic regime comparable to the dynamics of supramolecular host–guest systems. Interestingly, rotation around these systems'  $C=C$  double bond was already proposed by Dimroth and Criegee in 1957.<sup>28a</sup> Experimental evidence supporting this rotation, however, has remained scarce since the primarily studied symmetrically substituted systems ( $2 \times CN$  or  $2 \times COOR$ ) interconvert between degenerate conformations that cannot be distinguished by

<sup>a</sup> Faculty for Chemistry and Chemical Biology, TU Dortmund University, Otto-Hahn Str. 6, 44227 Dortmund, Germany. E-mail: [guido.clever@tu-dortmund.de](mailto:guido.clever@tu-dortmund.de)

<sup>b</sup> Institute for Inorganic Chemistry, Georg-August-University Göttingen, Tammannstr. 4, 37077 Göttingen, Germany

† Electronic supplementary information (ESI) available: Experimental procedures, characterization, NMR and mass spectra, X-ray crystallography and computational details. CCDC 1478914 and 1478915. For ESI and crystallographic data in CIF or other electronic format see DOI: 10.1039/c6cc04155h



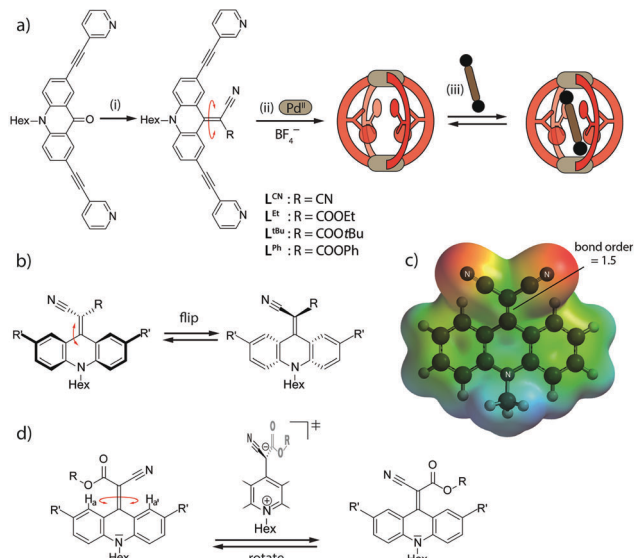


Fig. 1 (a) Ligand synthesis, cage assembly and guest uptake: (i) malonic acid derivative,  $TiCl_4$ , base,  $CH_2Cl_2$  (details see ESI†) (ii)  $L^R$ ,  $[Pd(CH_3CN)_4](BF_4)_2$ ,  $CD_3CN$ , (iii) bisulfonate guest ( $NBu_4$  salt). (b) Flipping of the endohedral attachments, (c) electrostatic potential map of the dicyano ligand  $L^{CN}$  highlighting the partial charge separation and  $C=C$  double-bond weakening in the push–pull backbone, (d) rotation of the endohedral functionality via a charge-separated transition state.

NMR methods. For one- or two-electron reduced molecules based on the same backbone, however, Akutagawa and Sutherland reported rotation.<sup>32</sup>

On the other hand, an internal motion that has already been described for such double-bonded compounds is flipping of the bent-out substituent between both faces of the backbone (Fig. 1b).<sup>32a</sup> We have observed a similar effect in the previously reported, electron rich adamantly system, but ruled out any thermally induced rotation around the  $C=C$  bond as evidenced by experimental and theoretical results.<sup>26</sup>

To the best of our knowledge, the rotation around the  $C=C$  double bond in non-reduced, unsymmetrically acceptor-substituted acridinylidene systems has never been reported (Fig. 1d). Furthermore, the use of such a push–pull endohedral functionality inside a self-assembled molecular cavity is unprecedented. In order to compare the dynamics of the rotor functionality in discrete ligands, self-assembled cages and their host–guest complexes we synthesized one symmetrically substituted ( $2 \times CN$ ) ligand  $L^{CN}$  and three unsymmetric derivatives  $L^R$  ( $R = Et, tBu$  or  $Ph$  esters; Fig. 1a). Variable temperature NMR studies in different solvents revealed that the unsymmetrically substituted ligands indeed show rotational dynamics around the  $C=C$  double bond depending on the conditions as evidenced by the splitting or coalescence of backbone protons  $H^a$  and  $H^{a'}$  (Fig. 2 and ESI†). As expected, rotation is accelerated at higher temperatures and in more polar solvents ( $MeOH > DMSO > MeNO_2 > MeCN > THF$ ) that better stabilize the charge-separated, twisted transition state (Fig. 1d and ESI†). Exemplarily, Fig. 2 compares NMR spectra of ligand  $L^{tBu}$  measured in THF at 198 K (Fig. 2a) and in acetonitrile at 298 K (Fig. 2b) with the former spectrum showing

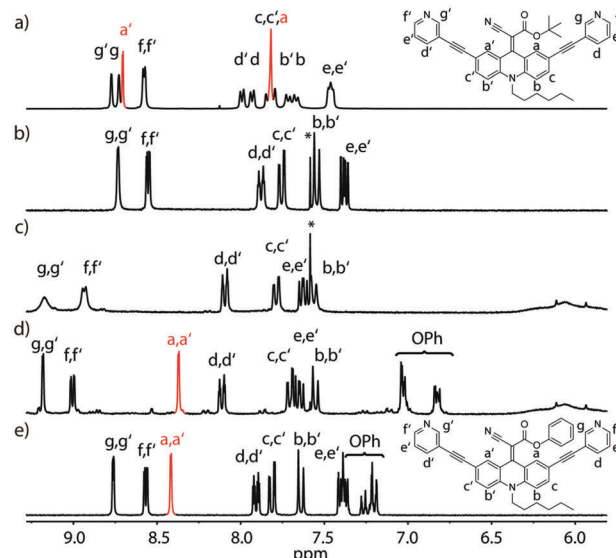


Fig. 2  $^1H$ -NMR spectra of ligands  $L^{tBu}$  and  $L^{Ph}$  and their corresponding  $[Pd_2L_4]$  cages. (a) Ligand  $L^{tBu}$  in THF (400 MHz, 198 K,  $d^8$ -THF), (b) ligand  $L^{tBu}$  in acetonitrile, (c) cage  $[Pd_2L^{tBu}_4]$ , (d) cage  $[Pd_2L^{Ph}_4]$  and (e) ligand  $L^{Ph}$  (400 MHz, 298 K,  $CD_3CN$ ). Aromatic protons closest to the spinning rotor are marked in red ( $a/a'$ ). Fast rotation results in one set of aromatic proton signals (e), slow rotation in two sets (a) and rotation with rates close to the NMR timescale in coalescence and signal broadening (b). \* =  $CHCl_3$ .

signal splitting for all aromatic protons, *i.e.* sharp resonances for protons  $H^a$  and  $H^{a'}$ , assignable to a locked conformation, and the latter spectrum revealing only one set of aromatic signals and complete broadening of  $H^a$  and  $H^{a'}$  protons, indicating fast rotation in the NMR coalescence regime.

Likewise, the rotation of the phenylester was found to be faster than the spinning observed in the more electron rich ethyl- and *t*-butyl-substituted ligands, as can be seen by comparing the spectra shown in Fig. 2b and e. The latter spectrum contains a single sharp signal assigned to the rapidly interchanging  $H^a$  and  $H^{a'}$  positions in the phenyl-substituted ligand. In addition, the low-temperature NMR measurements of ligand  $L^{Et}$  in THF reveal a splitting of the rotor's  $OCH_2CH_3$  signal due to desymmetrization into a diastereotopic pair of protons sitting next to an unusual element of chirality (a bent double bond carrying distinguishable substituents). Around 213 K, the onset of signal splitting hints at a rapid flipping motion of the endohedral substituent while the discussed rotation is already extremely slow at these low temperatures (Fig. 1b and ESI†).

A comparison of the UV-Vis spectra of all examined ligands further reveals that an increasing charge stabilization within the push–pull system goes along with increasing red-shift of the longest-wavelength maximum ( $tBu < Et < Ph < CN$ ; ESI†).

Regardless of their dynamic peculiarities, all ligands readily formed dinuclear  $[Pd_2L_4]$  coordination cages upon treatment with the palladium salt  $[Pd(CH_3CN)_4](BF_4)_2$  in acetonitrile as observed in the NMR spectra (Fig. 2c and d) and high-resolution ESI MS results (ESI†). Analogous to the behaviour of the free ligands, the spinning rates of the rotors inside the cages increase with increasing solvent polarity.



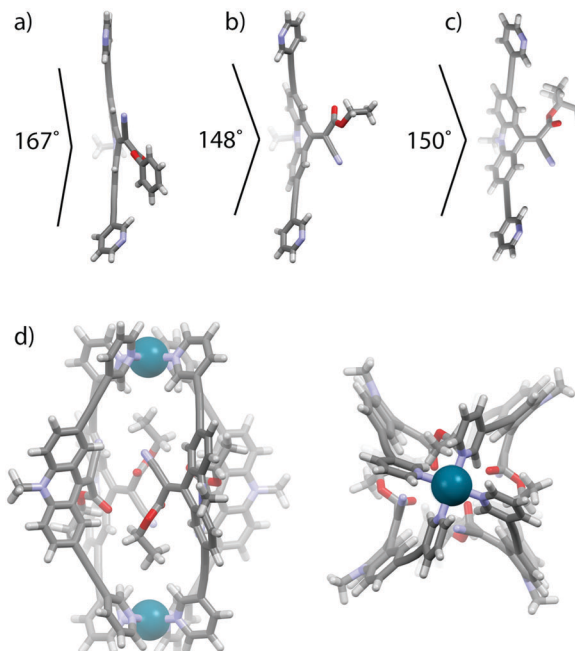


Fig. 3 (a) X-ray crystal structures of ligands (a)  $\mathbf{L}^{\text{Ph}}$  and (b)  $\mathbf{L}^{\text{Et}}$  and (c) DFT calculated structures of ligand  $\mathbf{L}^{\text{tBu}}$  and (d) the lowest energy conformer of cage  $[\text{Pd}_2\mathbf{L}^{\text{Et}}_4]$ .

Single crystal X-ray structures were obtained for ligands  $\mathbf{L}^{\text{Ph}}$  and  $\mathbf{L}^{\text{Et}}$  (Fig. 3a, b and ESI<sup>†</sup>). In comparison with a DFT calculated model of ligand  $\mathbf{L}^{\text{tBu}}$  (Fig. 3c), a substituent effect on the double-bond twisting and bending of the rotor moiety with respect to the backbone was clearly observed. The phenyl-substituted ester can stabilize negative charge density at the rotor-end of the double bond, hence leading to a rather large double bond twisting of  $23^\circ$  and a quite flat backbone structure ( $167^\circ$  internal bending). In contrast, the more electron rich ethyl and *tert*-butyl substituents lead to twists of only  $8^\circ$  and  $10^\circ$ , respectively, and more pronounced backbone bending ( $148^\circ$  and  $150^\circ$ ).

Since no crystals suitable for X-ray structure determination of the self-assembled cages could be obtained, we calculated the lowest energy conformations of cage  $[\text{Pd}_2\mathbf{L}^{\text{Et}}_4]$  by dispersion corrected DFT (B3LYP-D3/def2-SVP in PCM-acetonitrile) geometry optimizations (Fig. 3d, ESI<sup>†</sup>). In the two lowest energy conformers (differing by less than  $1 \text{ kcal mol}^{-1}$ ), the four unsymmetric endohedral attachments adopt a *trans*- or *cis*-up/down arrangement, respectively, with respect to the Pd–Pd axis. The calculation of the *cis*-conformer shown in Fig. 3d smoothly converged with a  $C_i$  symmetry in which two of the ethyl groups are slightly twisted away from the cage while the other two are oriented inside the cavity. A tentative arrangement with all four substituents showing in the direction of only one of the Pd centres was found to be of significant higher energy according to the calculations (ESI<sup>†</sup>).

Next, we examined changes of the dynamics of the rotor in dependence of its supramolecular surrounding by comparing the behaviour of the free ligand with the respective self-assembled cage and a host–guest complex. Fig. 4 summarizes the results for the  $\mathbf{L}^{\text{Et}}$  system. At room temperature (298 K) this ligand shows rotational dynamics with a rate close to the NMR timescale, thus the

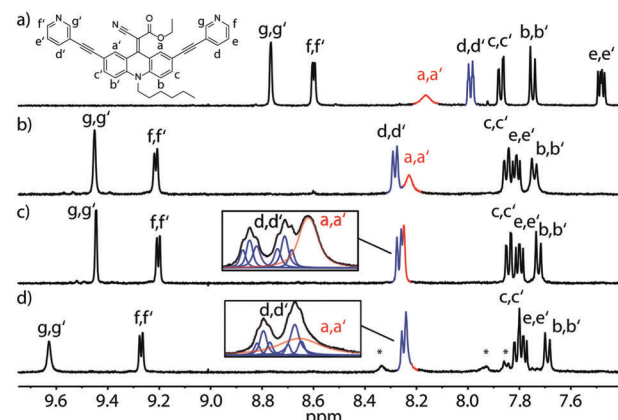


Fig. 4 <sup>1</sup>H-NMR spectra of (a) ligand  $\mathbf{L}^{\text{Et}}$ , (b) cage  $[\text{Pd}_2\mathbf{L}^{\text{Et}}_4]$  at 298 K, (c) the same cage at 333 K and (d) host–guest complex [guest@ $[\text{Pd}_2\mathbf{L}^{\text{Et}}_4]$ ] containing 1.0 eq. 2,7-naphthyl bisulfonate at 333 K (400 MHz, DMSO-d<sub>6</sub>). Cage formation and temperature increase leads to accelerated rotation and sharpening of the a/a' signal (red). Guest uptake slows down spinning of the endohedral rotor, as shown by line fitting analysis of deconvoluted signals d/d' (blue) and a/a' (red). \* = signals of the encapsulated guest.

spectrum shows a single, broadened resonance as an average for protons H<sup>a</sup> and H<sup>a'</sup> (Fig. 4a). Interestingly, assembly to the coordination cage results in a sharpening of this signal, indicating accelerated rotation, which we assume to be either caused by electronic changes in the conjugated system resulting from the coordination to the Pd(II) cations or by the cavity's special environment. As possible explanations for the latter effect we suggest an altered viscosity or polarity inside the cage confinement as compared to the free solution.

The signal further sharpens when the cage is heated to 333 K resulting from a thermally induced increase of the spinning frequency (Fig. 4c). Subsequently, we examined cage  $[\text{Pd}_2\mathbf{L}^{\text{Et}}_4]$  for the uptake of several anionic guest molecules (ESI<sup>†</sup>). A particularly interesting interaction was observed with the guest 2,7-naphthyl bisulfonate. In acetonitrile and nitromethane, this guest showed slow exchange on the NMR timescale, in DMSO it exhibited fast exchange, whilst in methanol, precipitation hampered the analysis. In the presence of the guest, the spectra measured at room temperature suffered from ample signal broadening which was partially resolved by conducting the measurements at 333 K (Fig. 4c, d and ESI<sup>†</sup>).

Most interestingly, a careful analysis of the overlapping NMR signals including the resonance of the a/a' protons revealed, that the encapsulation of one molecule 2,7-naphthyl bisulfonate slows down the spinning of the endohedral rotors, accompanied by typical downfield shifts for the cage protons in contact with the guest (Fig. 4d). This guest-induced “breaking effect” nicely complements our previous findings concerning the flipping motion in a related adamantyl cage.<sup>26</sup>

In conclusion, we reported a series of self-assembled coordination cages based on a new type of endohedral push–pull rotor whose rotational dynamics are influenced by the assembly process, solvent polarity and derivatization of the electron-withdrawing moieties. In addition, the presence of an encapsulated guest was found to slow down the rotation. We see potential uses for such



dynamic push–pull systems in the construction of stimuli responsive supramolecular systems, catalytic cavities and functional materials. Comparable sterically congested stilbene and imine derivatives based on tricyclic aromatic molecules featuring light-triggered rotation around C=C or C=N double-bonds have found remarkable application in supramolecular systems.<sup>33,34</sup> Currently, we examine the photochemical and redox behaviour of herein reported compounds with the aim to equip them with stimuli-responsive control elements.

This work was supported by the DFG through Grants CL 489/2-1, SPP 1807 and IRTG 1422. We thank Dr H. Frauendorf (Georg-August University Göttingen) for measuring the ESI mass spectra and Rene Rieger, Dr Michael John and Dr Wolf Hiller (TU Dortmund) for their help with the NMR experiments.

## Notes and references

- 1 A. Liljas, L. Liljas, J. Piskur, G. Linblom, P. Nissen and M. Kjeldgaard, *Textbook of Structural Biology*, World Scientific Publishing, Singapore, 2009.
- 2 J.-P. Changeux and S. J. Edelstein, *Science*, 2005, **308**, 1424–1428.
- 3 (a) L. Palmer and J. Rebek, *Org. Biomol. Chem.*, 2004, **2**, 3051–3059; (b) M. D. Pluth and K. N. Raymond, *Chem. Soc. Rev.*, 2007, **36**, 161–171.
- 4 E. Persch, O. Dumele and F. Diederich, *Angew. Chem., Int. Ed.*, 2015, **54**, 3290–3327.
- 5 M. Yoshizawa, J. K. Klosterman and M. Fujita, *Angew. Chem., Int. Ed.*, 2009, **48**, 3418–3438.
- 6 V. Croué and S. Goeband M. Sallé, *Chem. Commun.*, 2015, **51**, 7275–7289.
- 7 (a) M. Han, R. Michel, B. He, Y.-S. Chen, D. Stalke, M. John and G. H. Clever, *Angew. Chem., Int. Ed.*, 2013, **52**, 1319–1323; (b) M. Han, Y. Luo, B. Damaschke, L. Gómez, X. Ribas, A. Jose, P. Peretzki, M. Seibt and G. H. Clever, *Angew. Chem., Int. Ed.*, 2016, **55**, 445–449.
- 8 A. J. McConnell, C. S. Wood, P. P. Neelakandan and J. Nitschke, *Chem. Rev.*, 2015, **115**, 7729–7793.
- 9 L. Kovbasyuk and R. Krämer, *Chem. Rev.*, 2004, **104**, 3161–3187.
- 10 J. Wang and B. L. Feringa, *Science*, 2011, **331**, 1429–1432.
- 11 C. Piguet, G. Bernardinelli and G. Hopfgartner, *Chem. Rev.*, 1997, **97**, 2005–2062.
- 12 (a) J. E. Beves, B. A. Blight, C. J. Campbell, D. A. Leigh and R. T. McBurney, *Angew. Chem., Int. Ed.*, 2011, **50**, 9260–9327; (b) R. S. Forgan, J.-P. Sauvage and J. F. Stoddart, *Chem. Rev.*, 2011, **111**, 5434–5464.
- 13 (a) M. Fujita, K. Umemoto, M. Yoshizawa, N. Fujita, T. Kusukawa and K. Biradha, *Chem. Commun.*, 2001, 509–518; (b) S. J. Dalgarno, P. Power and J. L. Atwood, *Coord. Chem. Rev.*, 2008, **252**, 825–841; (c) R. Chakrabarty, P. S. Mukherjee and P. J. Stang, *Chem. Rev.*, 2011, **111**, 6810–6918; (d) R. Custelcean, *Chem. Soc. Rev.*, 2014, **43**, 1813–1824; (e) M. Han, D. M. Engelhard and G. H. Clever, *Chem. Soc. Rev.*, 2014, **43**, 1848–1860.
- 14 M. M. J. Smulders, I. A. Riddell, C. Browne and J. R. Nitschke, *Chem. Soc. Rev.*, 2013, **42**, 1728–1754.
- 15 C. Desmaerts, G. Gontard, A. L. Cooksy, M. N. Rager and H. Amouri, *Inorg. Chem.*, 2014, **53**, 4287–4294.
- 16 J. E. M. Lewis, E. L. Gavey, S. A. Cameron and J. D. Crowley, *Chem. Sci.*, 2012, **3**, 778–784.
- 17 (a) M. Tominaga, K. Suzuki, T. Murase and M. Fujita, *J. Am. Chem. Soc.*, 2005, **127**, 11950–11951; (b) K. Suzuki, M. Kawano, S. Sato and M. Fujita, *J. Am. Chem. Soc.*, 2007, **129**, 10652–10653; (c) T. Murase, S. Sato and M. Fujita, *Angew. Chem., Int. Ed.*, 2007, **46**, 1083–1085.
- 18 (a) A. M. Johnson, O. Moshe, A. S. Gamboa, B. W. Langloss, J. F. K. Limtiaco, C. K. Larive and R. J. Hooley, *Inorg. Chem.*, 2011, **50**, 9430–9442; (b) A. M. Johnson and R. J. Hooley, *Inorg. Chem.*, 2011, **50**, 4671–4673; (c) M. C. Young, A. M. Johnson, A. S. Gamboa and R. J. Hooley, *Chem. Commun.*, 2013, **49**, 1627–1629; (d) Q.-Q. Wang, S. Gonell, S. H. A. M. Leenders, M. Dürr, I. Ivanović-Burmazović and J. N. H. Reek, *Nat. Chem.*, 2016, **8**, 225–230.
- 19 P. Howlader, P. Das, E. Zangrandi and P. S. Mukherjee, *J. Am. Chem. Soc.*, 2016, **138**, 1668–1676.
- 20 (a) M. D. Johnstone, E. K. Schwarze, G. H. Clever and F. M. Pfeffer, *Chem. – Eur. J.*, 2015, **21**, 3948–3955; (b) S. Bandi, A. K. Pal, G. S. Hanan and D. K. Chand, *Chem. – Eur. J.*, 2014, **20**, 13122–13126; (c) R. Saalfrank, V. Seitz, D. L. Caulder, K. Raymond, M. Teichert and D. Stalke, *Eur. J. Inorg. Chem.*, 1998, 1313–1317.
- 21 S. Kubik, *Top. Curr. Chem.*, 2012, **319**, 1–34.
- 22 (a) S. J. Loeb, *Chem. Commun.*, 2005, 1511–1518; (b) V. N. Vukotic, K. J. Harris, K. Zhu, R. W. Schurko and S. J. Loeb, *Nat. Chem.*, 2012, **4**, 456–460.
- 23 (a) S. Kitagawa and K. Uemura, *Chem. Soc. Rev.*, 2005, **34**, 109–119; (b) A. Schneemann, V. Bon, I. Schwedler, I. Senkovska, S. Kaskel and R. A. Fischer, *Chem. Soc. Rev.*, 2014, **43**, 6062–6096; (c) Z.-J. Lin, J. Lu, M. Hong and R. Cao, *Chem. Soc. Rev.*, 2014, **43**, 5867–5895; (d) X. Jiang, B. Rodriguez-Molina, N. Nazarian and M. A. Garcia-Garibay, *J. Am. Chem. Soc.*, 2014, **136**, 8871–8874.
- 24 H.-B. Yang, K. Ghosh, B. H. Northrop, Y.-R. Zheng, M. M. Lyndon, D. C. Muddiman and P. J. Stang, *J. Am. Chem. Soc.*, 2007, **129**, 14187–14189.
- 25 S. P. Black, A. R. Stefankiewicz, M. M. J. Smulders, D. Sattler, C. A. Schalley, J. R. Nitschke and J. K. M. Sanders, *Angew. Chem., Int. Ed.*, 2013, **52**, 5749–5752.
- 26 S. Löffler, J. Lübben, A. Wuttke, R. A. Mata, M. John, B. Dittrich and G. H. Clever, *Chem. Sci.*, 2016, **7**, 4676–4684.
- 27 S. Löffler, J. Lübben, L. Krause, D. Stalke, B. Dittrich and G. H. Clever, *J. Am. Chem. Soc.*, 2015, **137**, 1060–1063.
- 28 (a) O. Dimroth and R. Criegee, *Chem. Ber.*, 1957, **90**, 2207–2215; (b) O. Tsuge, *Bull. Chem. Soc. Jpn.*, 1973, **46**, 283–285.
- 29 W. Chen, S. Wang, G. Yang, S. Chen, K. Ye, Z. Hu, Z. Zhang and Y. Wang, *J. Phys. Chem. C*, 2016, **120**, 587–597.
- 30 W.-C. Chow, G.-J. Zhou and W.-Y. Wong, *Macromol. Chem. Phys.*, 2007, **208**, 1129–1136.
- 31 M. Beyer, J. Fritscher, E. Feresin and O. Schiemann, *J. Org. Chem.*, 2003, **68**, 2209–2215.
- 32 (a) T. Takeda, H. Sugihara, Y. Suzuki, J. Kawamata and T. Akutagawa, *J. Org. Chem.*, 2014, **79**, 9669–9677; (b) K. D. Thériault, C. Radford, M. Parvez, B. Heyne and T. C. Sutherland, *Phys. Chem. Chem. Phys.*, 2015, **17**, 20903–20911.
- 33 (a) N. Koumura, R. W. Zijlstra, R. A. van Delden, N. Harada and B. L. Feringa, *Nature*, 1999, **401**, 152–155; (b) A. A. Kulago, E. M. Mes, M. Klok, A. Meetsma, A. M. Brouwer and B. L. Feringa, *J. Org. Chem.*, 2010, **75**, 666–679.
- 34 L. Greb and J.-M. Lehn, *J. Am. Chem. Soc.*, 2014, **136**, 13114–13117.

